Supporting Information

Electronic Devices Based on Oxide Thin Films Fabricated by Fibers-to-film Process

You Meng,[a,b] Ao Liu,[a,b] Zidong Guo,[a,b] Guoxia Liu,[a,b] Byoungchul Shin,[c] Yong-Young Noh,[d] Elvira Fortunato,[e] Rodrigo Martins[e] and Fukai Shan[a,b*]*

[a]College of Physics, Qingdao University, Qingdao 266071, China

[b]College of Electronic & Information Engineering, Qingdao University, Qingdao 266071, China

[c]Electronic Ceramics Center, Dong-Eui University, Busan 614-714, Korea

[d]Department of Energy and Materials Engineering, Dongguk University, Seoul 100-715, Korea

[e]Department of Materials Science/CENIMAT-I3N, Faculty of Sciences and Technology, New University of Lisbon and CEMOP-UNINOVA, Campus de Caparica, 2829-516 Caparica, Portugal

Corresponding author

* To whom correspondence should be addressed.

*E-mail: gxliu@qdu.edu.cn; fukaishan@yahoo.com

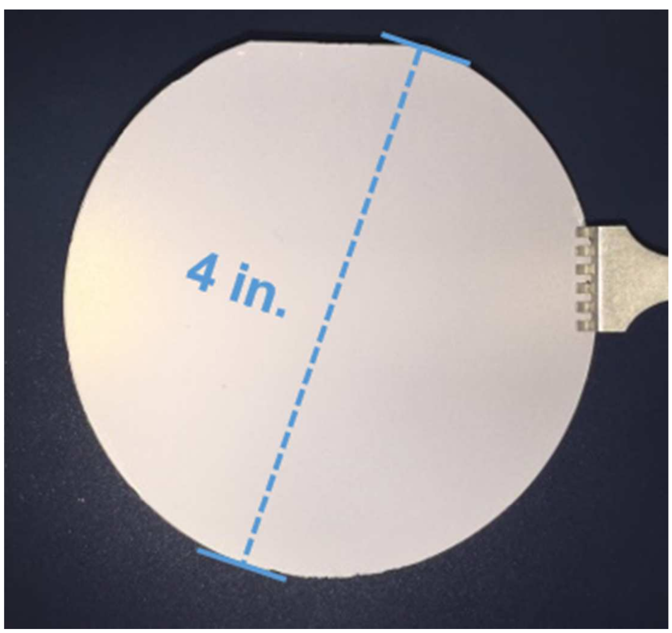

Figure S1. Photograph of as-spun In^{3+}/PLA nanofibers based on a 4 in. SiO_2/Si wafer.

[*]Corresponding author: gxliu@qdu.edu.cn; fukaishan@yahoo.com

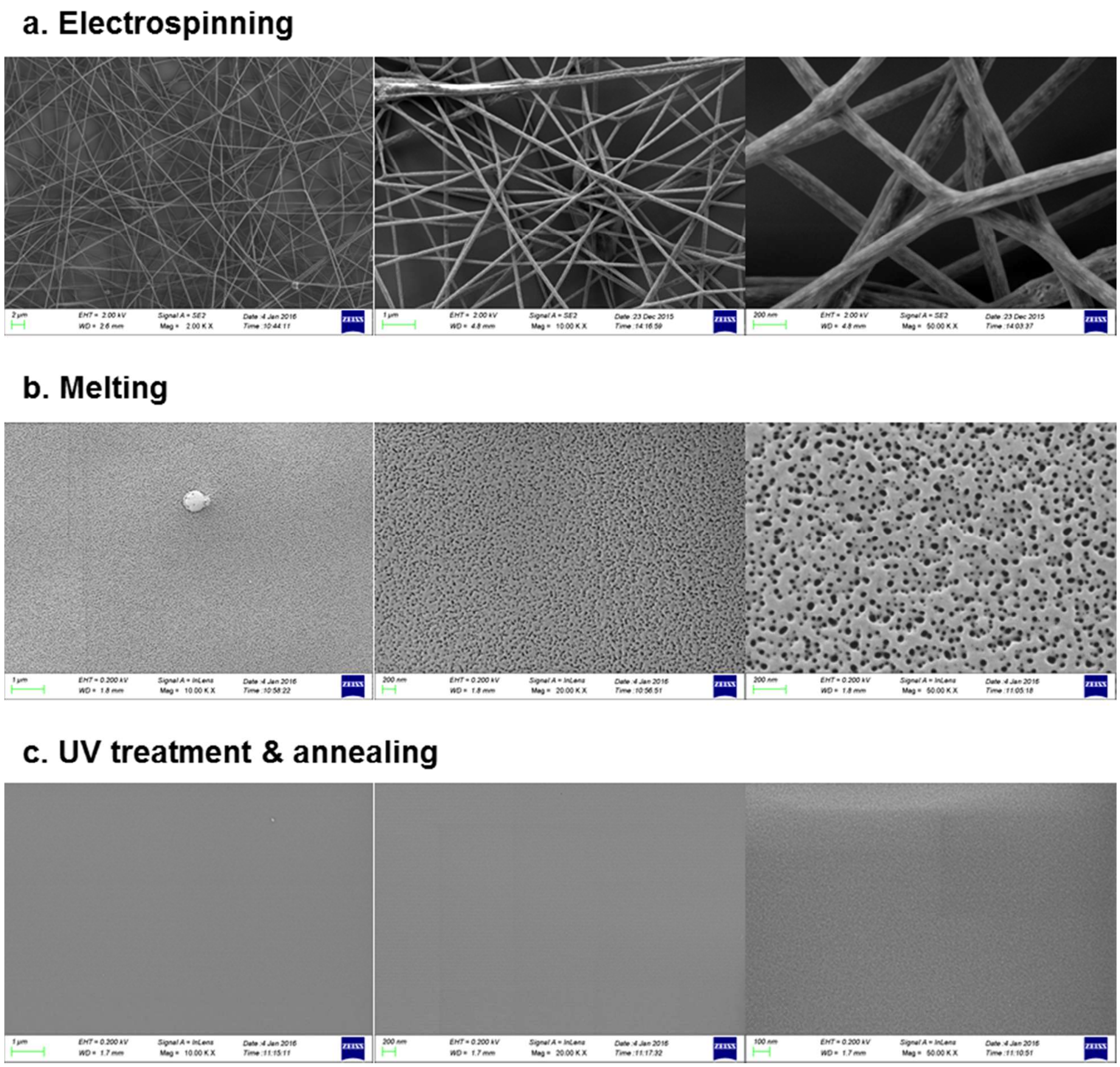

Figure S2. The morphological characteristics of **(a)** as-spun In^{3+}/PLA nanofibers, **(b)** melted In_2O_3 thin films, and **(c)** melted In_2O_3 thin films after UV treatment and thermally annealing at 350 ^oC.

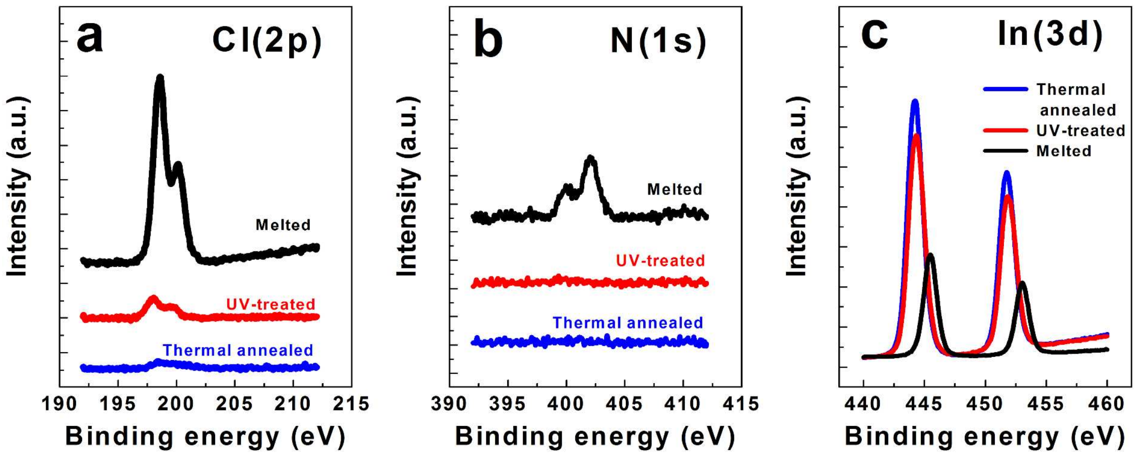

Figure S3. XPS **(a)** Cl(2p), **(b)** N(1s), and **(c)** In(3d) peak analysis of In_2O_3 thin films after being melted, after UV treatment, and after UV treatment followed by thermally annealing at 350 ^{o}C.

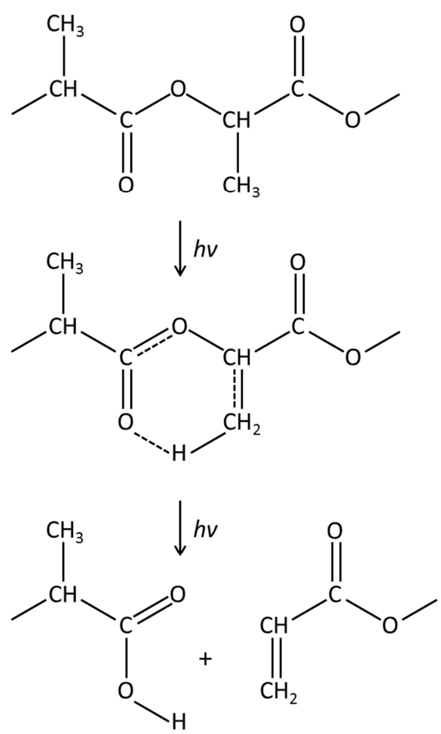

Figure S4. Norrish II type photochemical reaction in PLA. As a result of the photon-induced molecule excitation, the hydrogen atom of methyl group interacts with the oxygen atom of carbonyl, and the cyclic six-member intermediate is formed. The secondary bonds of cyclic six-member intermediate possess a dissociation energy of 0.5~10 kcal/mol, which is much lower than 200 kcal/mol of covalent intermolecular bonds. Therefore, these weak secondary bonds can be easily split by UV irradiation.

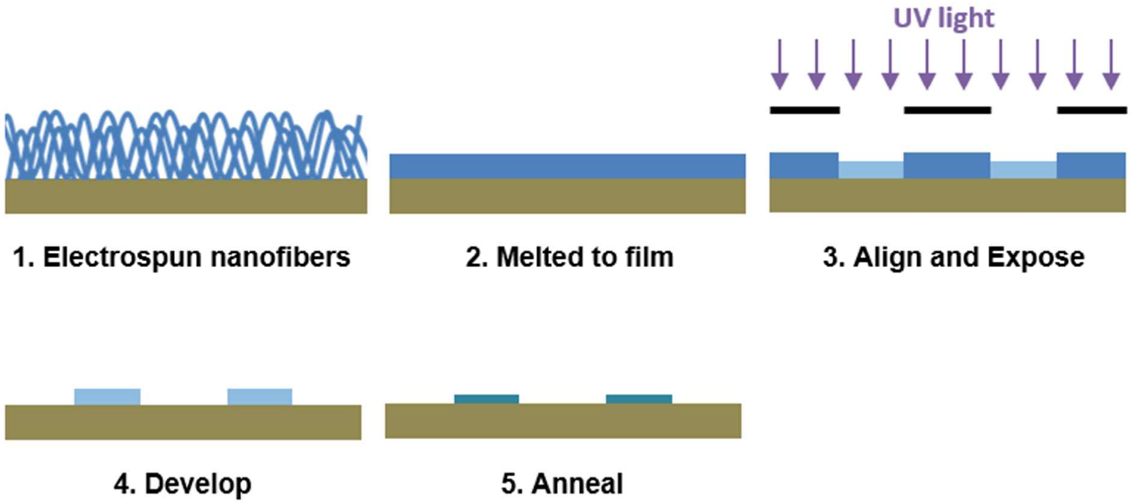

Figure S5. Flow diagram of the photoresist-free photolithography process.

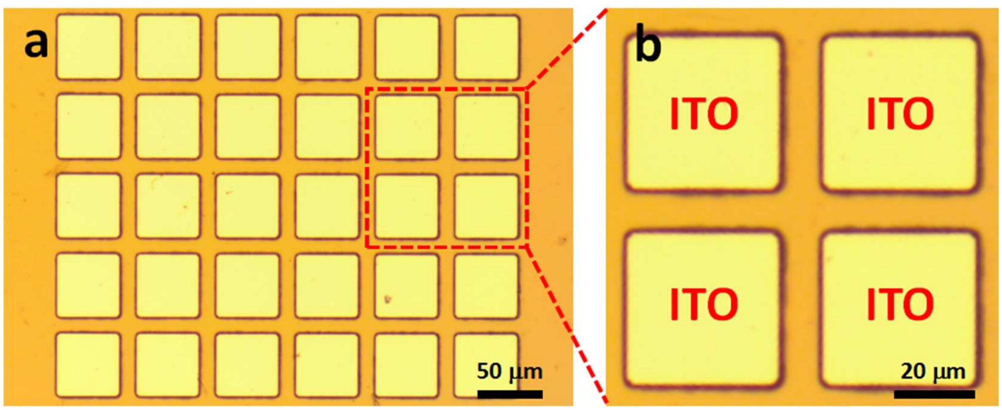

Figure S6. (a) Optical image and **(b)** the corresponding enlarged image of InSnO (ITO) thin films patterned by photoresist-free lithography.

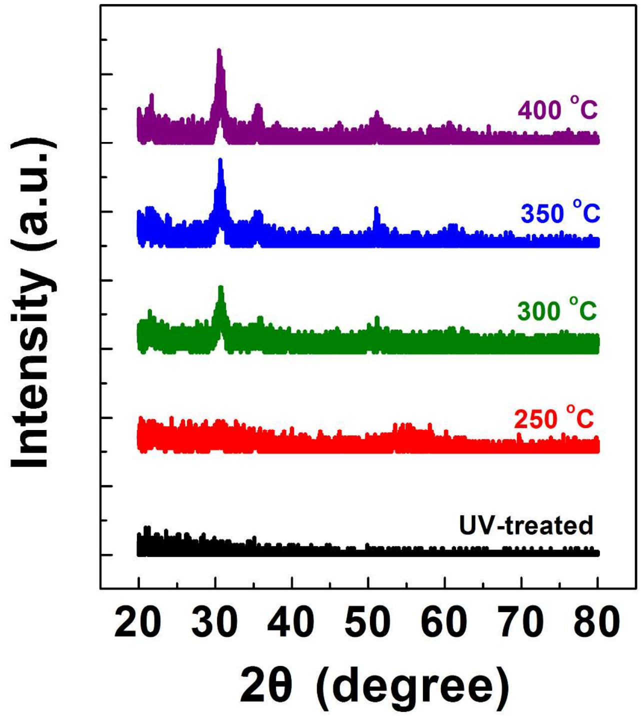

Figure S7. XRD patterns of FTF-processed In_2O_3 thin films (thickness: 100 nm) annealed at various temperatures (T_a).

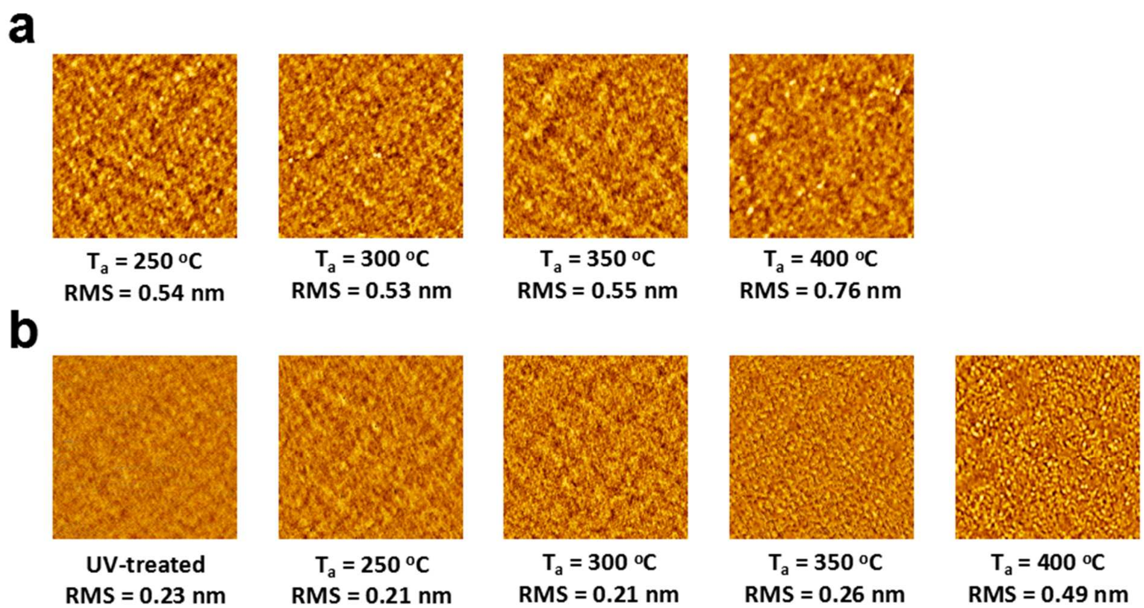

Figure S8. AFM images (1×1μm) of In_2O_3 thin films (thickness: 20 nm) annealed at various T_a **(a)** without and **(b)** with UV treatment.

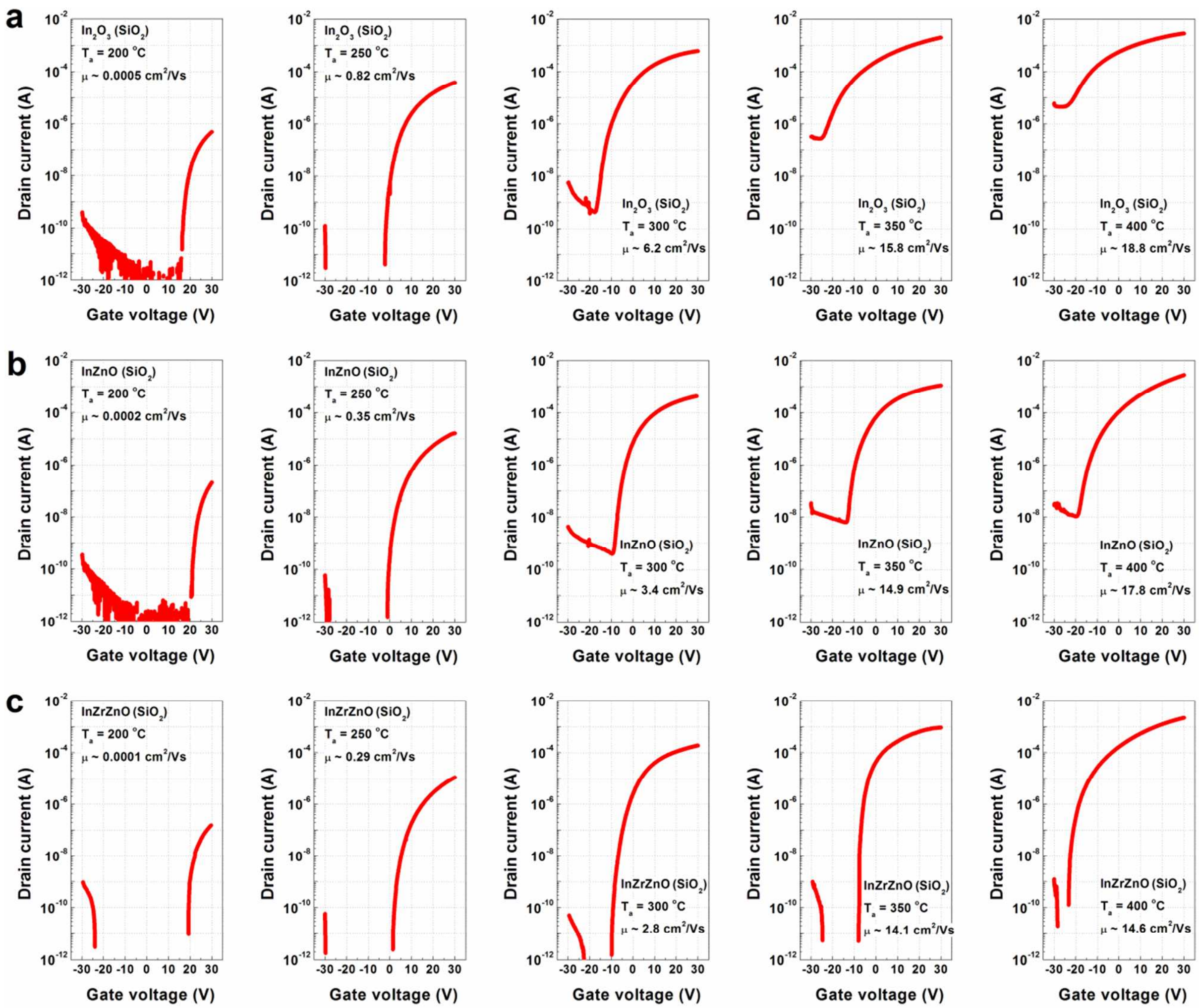

Figure S9. Transfer characteristics and corresponding mobilities of FTF-processed **(a)** In_2O_3, **(b)** InZnO and **(c)** InZrZnO TFTs based on SiO_2 dielectric layers annealed at various T_a. The thicknesses of the channel layers are 20 nm; source-drain voltage (V_D) is 30 V. The channel length and width for all the devices are 100 μm and 1000 μm, respectively.

Table S1 Electrical parameters of FTF-processed In_2O_3, InZnO and InZrZnO TFTs based on SiO_2 dielectric layers annealed at various T_a.

Metal oxide	*T_a (°C)*	*Mobility ($cm^2V^{-1}s^{-1}$)*	*I_{on}/I_{off}*	*V_{TH} (V)*
In_2O_3	***200***	Inactive (μ ~ 0.0005)*		
	250	0.82	~ 10^7	~ 13
	300	6.2	~ 10^6	~ 0
	350	15.8	~10^4	~ -1
	400	18.8	~ 10^3	~ -8
InZnO	***200***	Inactive (μ~0.0002)*		
	250	0.35	~ 10^7	~ 15
	300	3.4	~ 10^7	~ 3
	350	14.9	~ 10^6	~ -2
	400	17.8	~ 10^5	~ -5
InZrZnO	***200***	Inactive (μ~0.0002)*		
	250	0.29	~ 10^7	~ 17
	300	2.8	~ 10^8	~ 3
	350	14.1	~ 10^9	~ 0
	400	14.6	~ 10^8	~ -5

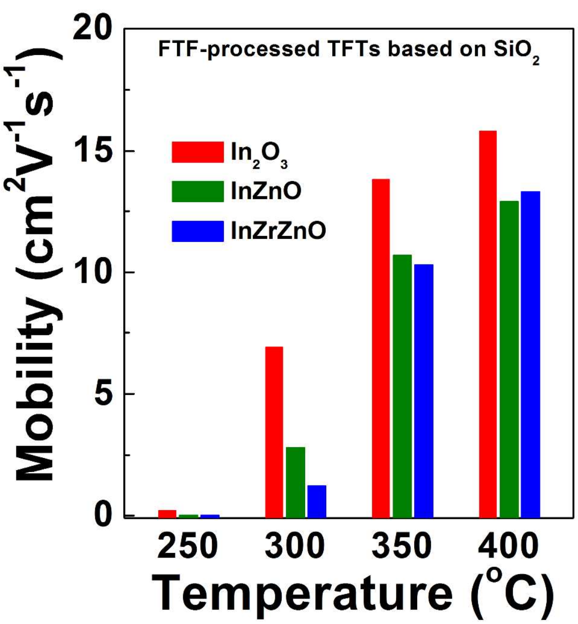

Figure S10. Mobility distribution of FTF-processed TFTs based on SiO_2 dielectric layers annealed at various T_a.

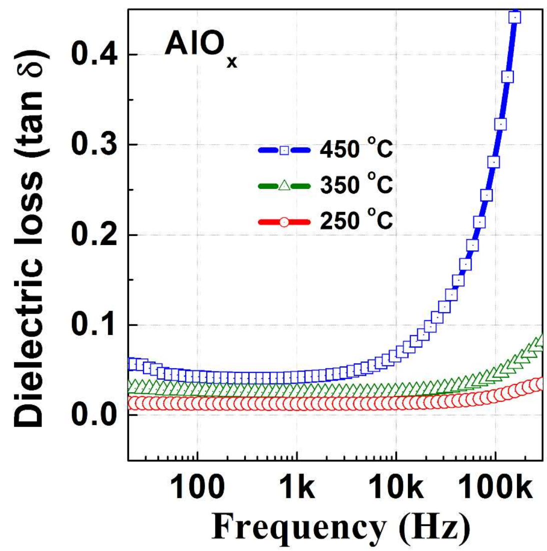

Figure S11. Dielectric losses (tan δ) of the FTF-processed AlO_x dielectric layers as functions of frequency measured at room temperature.

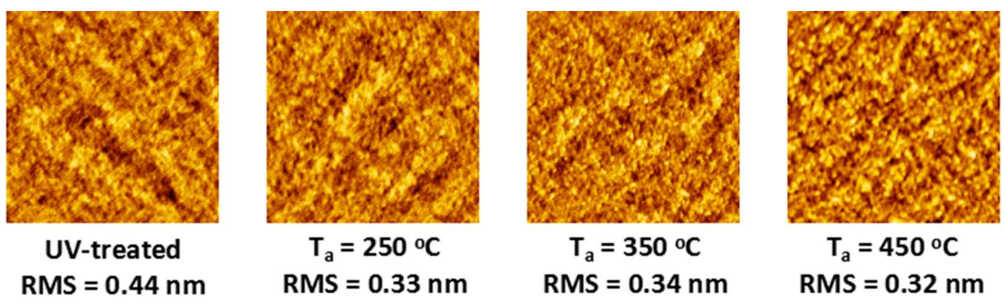

Figure S12. AFM images (1×1μm) of FTF-processed AlO_x thin films annealed at various T_a.

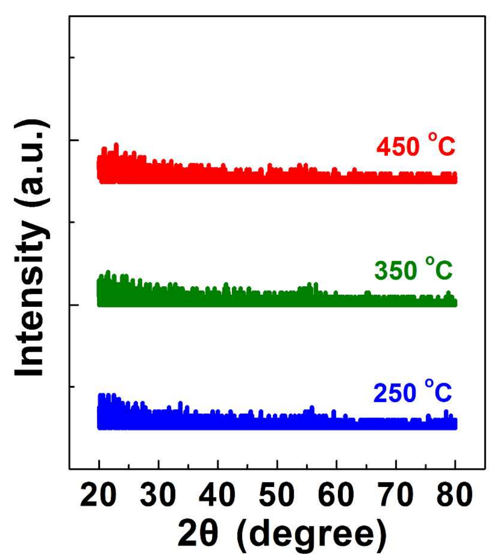

Figure S13. XRD patterns of FTF-processed AlO_x dielectric layers annealed at various T_a.

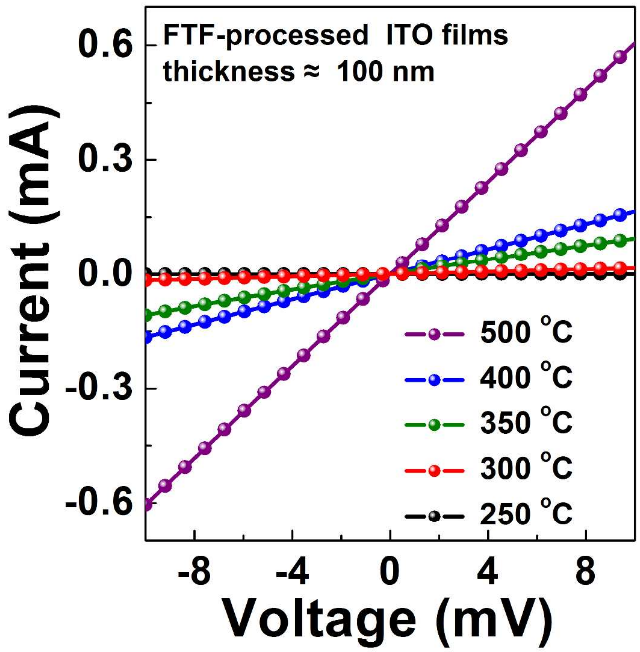

Figure S14. I-V characteristics of FTF-processed ITO films (In:Sn = 90:10, thickness: 100 nm) annealed at various T_a.

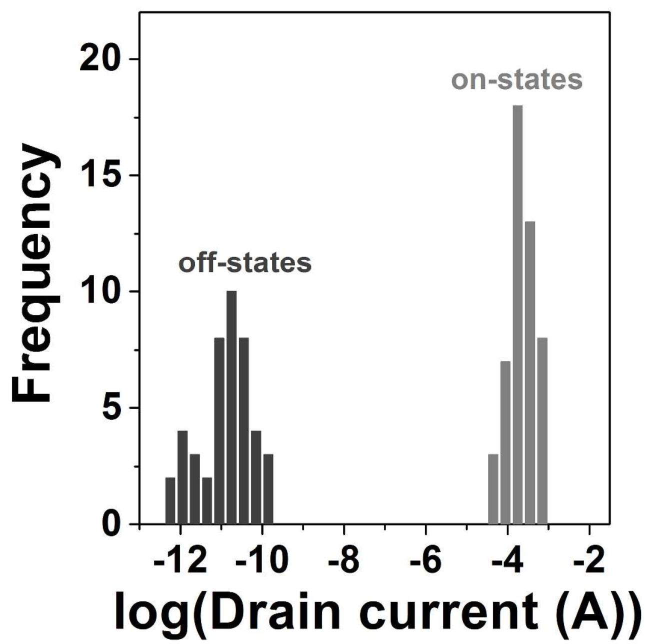

Figure S15. Histogram of on-state current and off-state current of 49 fully-FTF-processed In_2O_3/AlO_x TFTs.

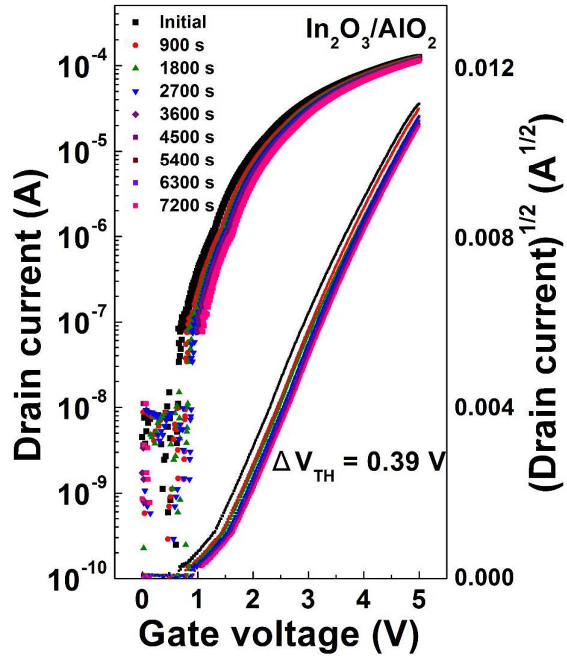

Figure S16. Transfer characteristics of fully-FTF-processed In_2O_3/AlO_x TFTs under PBS test for 7200 s.

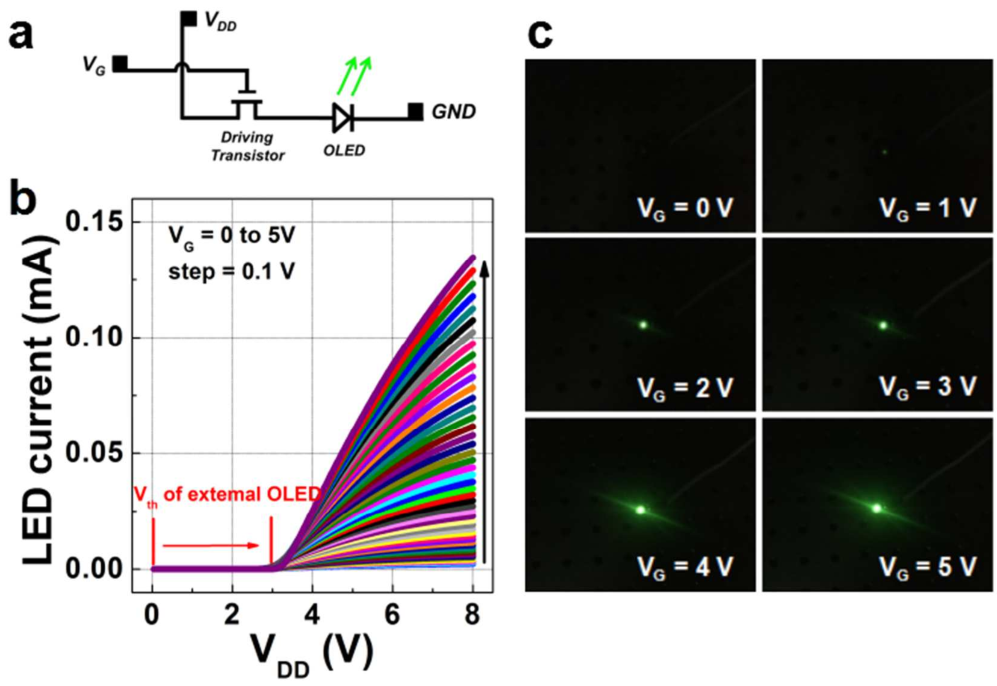

Figure S17. (a) Schematic diagram of one-transistor pixel circuit driven by fully FTF-processed In_2O_3/AlO_x TFTs. **(b)** Output characteristic of single pixel circuit, where the current flow through the LED (I_{LED}) is measured by sweeping the supply voltage (V_{DD}) while V_G ranging from 0 to 5 V with 0.1 V step. **(c)** Photographs of LED with various light intensities modulated by fully-FTF-processed In_2O_3/AlO_x TFTs ($V_{DD} = 6$ V).

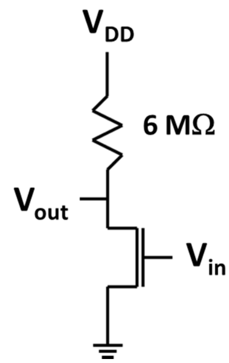

Figure S18. The circuit schematic of the resistor-loaded inverter based on fully-FTF-processed In_2O_3/AlO_x TFTs.

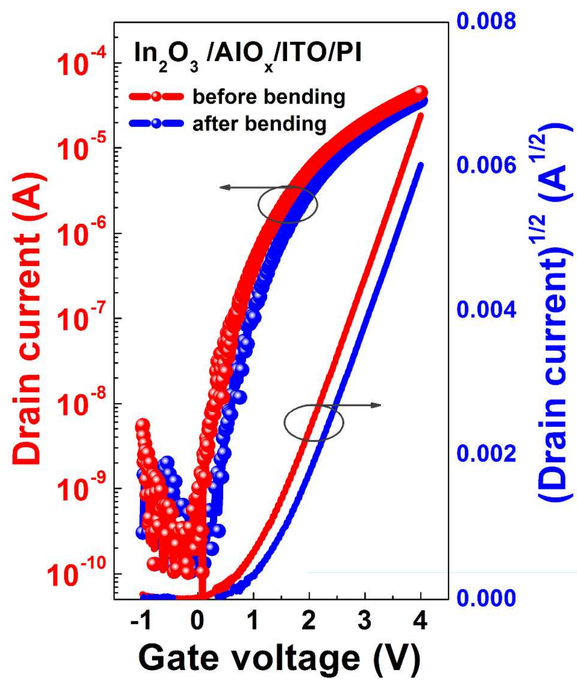

Figure S19. Transfer curves of the flexible In_2O_3/AlO_x TFTs before and after 100 cycles bending.